2016

Elucidation of the Fe(III) Gallate Structure in Historical Iron Gall Ink

Ponce, Also

Ponce, Aldo, et al. "Elucidation of the Fe (III) Gallate Structure in Historical Iron Gall Ink." Analytical chemistry 88.10 (2016): 5152-5158.
http://hdl.handle.net/10945/48737

analytical chemistry

Article

pubs.acs.org/ac

Elucidation of the Fe(III) Gallate Structure in Historical Iron Gall Ink

Aldo Ponce,[†] Lynn B. Brostoff,[*,‡] Sarah K. Gibbons,[†] Peter Zavalij,[†] Carol Viragh,[§] Joseph Hooper,[∥] Sufian Alnemrat,[∥] Karen J. Gaskell,[*,†] and Bryan Eichhorn[*,†]

[†]Department of Chemistry and Biochemistry, University of Maryland, College Park, Maryland 20742, United States

[‡]Preservation Research and Testing Division, Library of Congress, 101 Independence Avenue SE, Washington, District of Columbia 20540, United States

[§]Vitreous State Laboratory (VSL), The Catholic University of America, 400 Hannan Hall, 620 Michigan Avenue NE, Washington, District of Columbia 20064, United States

[∥]Department of Physics, Naval Postgraduate School at Monterey, Monterey, California 93943, United States

Supporting Information

ABSTRACT: Synthetic, structural, spectroscopic and aging studies conclusively show that the main colorant of historical iron gall ink (IGI) is an amorphous form of Fe(III) gallate·xH_2O (x = ~1.5−3.2). Comparisons between experimental samples and historical documents, including an 18th century hand-written manuscript by George Washington, by IR and Raman spectroscopy, XRD, X-ray photoelectron spectroscopy, and Mössbauer spectroscopy confirm the relationship between the model and authentic samples. These studies settle controversy in the cultural heritage field, where an alternative structure for Fe(III) gallate has been commonly cited.

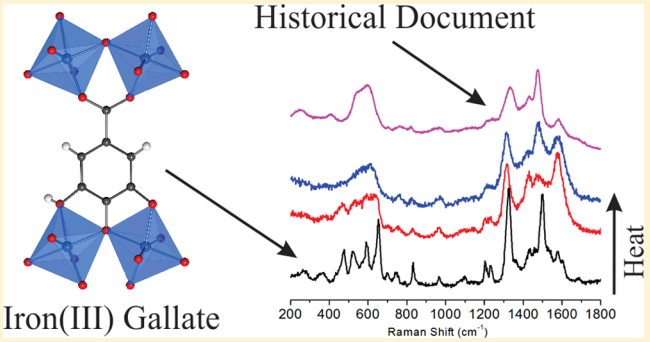

Prior to the 20th century, historical iron gall ink (IGI) was by far the most common writing material of the western world, and a plethora of recipes from which to produce the ubiquitous dark, brown-black ink can be found starting from at least the Middle Ages. This ink has been used to pen many of the most important documents and drawings in human history, including unique, hand-written works such as Thomas Jefferson's original draft of the Declaration of Independence, Abraham Lincoln's first draft of the Emancipation Proclamation, and Beethoven's original scores. While the virtue of IGI lies in its relative permanence, the great vice of this medium lies in its well-known tendency to degrade paper and parchment substrates.[1−7]

Despite its historical importance, there is little consensus on the chemical structure or composition of the iron-gallate complex, the main species responsible for the color of the IGI. We describe here a series of synthetic, structural, spectroscopic, and aging studies, which unequivocally demonstrate that the primary colorant in IGI is an amorphous form of an octahedral Fe(III) gallate metal organic framework structure that has previously been described by Wunderlich[8−10] and Feller.[11] Unlike the majority of prior studies, we use authentic IGI precursors to prepare both crystalline and amorphous forms of the IGI precipitate and study the crystal-to-amorphous transition by way of XRD, thermal gravimetric analysis (TGA), IR and Raman, Mössbauer, and X-ray photoelectron spectroscopy (XPS). Spectroscopic comparisons with historical documents prove the relevance of the synthetic crystalline and amorphous forms of the model IGI materials to those found in the authentic manuscripts.

Historical IGI recipes typically contain three basic ingredients: Fe(II) sulfate, gallic acid from hydrolyzed tannins, and a resin or polysaccharide such as gum arabic that functions as a binder, emulsifying agent, and a dispersing or viscosity increasing agent.[2,12−15] While it is widely accepted that the IGI colorant results from a reaction of aqueous Fe(II) and gallic acid,[2,9,16−19] the structure and composition of the resulting iron-gallate complex are controversial. Characterization of the dark blue-black precipitate that initially forms in these reactions has been hampered by its amorphous nature and the presence of impurity phases typically found in historical recipes that complicate analytical evaluation.

A number of studies have attempted to describe the structure and composition of the iron-gallate complex,[8−11,18−26] but only two studies are commonly referenced in the field of cultural heritage. In the first of these, Wunderlich et al. demonstrated in 1990 that the reaction between gallic acid and Fe(III) chloride gives an amorphous blue-black, insoluble polymeric material along with a few black crystals of the Fe(III) gallate coordination polymer, $Fe(C_7O_5H_3)\cdot 2H_2O$.[8−10] However, because Wunderlich's complex was synthesized from an Fe(III) chloride precursor, there is general and explicit skepticism in

Received: January 8, 2016
Accepted: April 8, 2016

DOI: 10.1021/acs.analchem.6b00088
Anal. Chem. XXXX, XXX, XXX−XXX

cultural heritage community regarding its relevance.[2,27−29] In 2006, Feller and Cheetham obtained bluish-black, rod-shaped crystals of the same complex using hydrothermal methods and equal molar ratios of Fe(II) chloride and gallic acid precursors,[11] but this work remains largely unacknowledged in the cultural heritage literature.

In the second study, published in 1999, Krekel proposed an alternative model based on experiments involving the reaction between equal molar ratios of traditional IGI starting materials: Fe(II) sulfate and gallic acid.[23,24] The author proposed that an initial oxidation of the Fe(II) precursor occurs to form a tetrahedral Fe(III) bis-gallate complex, which undergoes further decarboxylation of the gallate ligands to produce a black, insoluble Fe(III) octahedral pyrogallin complex, $Fe_2(C_6O_3H_3)_2 \cdot 4H_2O$ (Figure S1). Although there is little structural or spectroscopic evidence to support these proposals, Krekel's Fe(III) octahedral pyrogallin complex has been widely accepted as the true colorant of IGI in the cultural heritage and scientific literature.[27,28,30−35] In this study, we show that an amorphous form of the Wunderlich complex is indeed formed in authentic IGI and is its primary colorant.

EXPERIMENTAL SECTION

Synthesis of IGI Precipitate. The reaction of gallic acid with Fe(II) sulfate results in the formation of a dark blue-black solution that deposits a dark blue-black precipitate over time. The precipitate, denoted as the IGI precipitate (IGI-ppt), was prepared in three molar ratios: 1:1, 3:1, and 1:3 gallic acid to Fe(II) sulfate, respectively. For a 1:1 molar ratio preparation, 2.35 mmol (442 mg) of gallic acid monohydrate (Sigma-Aldrich, > 98%) was completely dissolved in 40 mL of deionized water through sonication at 40 °C; the pH of the solution was 2.85. Subsequently, 2.35 mmol (654 mg) of Fe(II) sulfate heptahydrate (Sigma-Aldrich, >99%) was added to the stirred gallic acid solution. After a week of stirring in air, a very dark blue-black precipitate separated from solution by centrifugation at 4 °C at a speed of 12 000 rpm for 15 min. The supernatant was collected and the precipitate was washed with water and centrifuged twice to remove unreacted starting materials and impurities. The isolated precipitate was then dried under vacuum and stored for further analysis.

Synthesis of Crystalline Fe(III) Gallate. Hydrothermal reaction conditions similar to those of Feller and Cheetham[11] were used to produce crystalline samples of the iron-gallate. In the optimal reaction, 1.00 mmol (188 mg) of gallic acid monohydrate (Sigma-Aldrich, >98%) was dissolved in 10 mL of 0.050 M potassium hydroxide (Sigma-Aldrich, >85%) solution; the pH of the resulting solution was ∼4.50. Then 1.00 mmol (278 mg) of Fe(II) sulfate heptahydrate (Sigma-Aldrich, >99%) was added to the gallic acid solution. The reaction mixture was stirred until all reactants were completely dissolved and sealed in a Teflon-lined Parr acid digestion bomb, then heated at 125 °C under autogenous pressure for 48 h. The reaction vessel was cooled to room temperature and the black crystals were washed several times with deionized water, dried in air, and stored for further analysis.

Thermogravimetric Studies. Thermogravimetric analysis (TGA) results were obtained with a TA Instruments Q600; the samples were heated from room temperature at a rate of 10 °C/min up to a 120 °C, held for 20 min, and heated to 300 °C at 10 °C/min in a nitrogen atmosphere.

Infrared Studies. Fourier transform-infrared (FT-IR) spectroscopy studies were carried out with a Thermo Nicolet 670 equipped with an attenuated total reflectance (ATR) accessory using a ZnSe crystal plate. The samples were measured directly without any preparation.

X-ray Diffraction Studies. The single crystal data were measured on a Bruker Smart Apex2 diffractometer equipped with CCD area detector using Mo Kα radiation from sealed tube, a graphite monochromator, and 0.5 mm monocap collimator. The intensities of 9018 reflections were integrated from 2230 frames measured with a step of 0.3° 2θ and an exposure of 60 s. The integral intensities were corrected for absorption and Lorenz-polarization factors.

Powder diffraction data were collected on a C2/D8 Bruker Discover diffractometer equipped with a Vantec 500 area detector using Cu Kα radiation from sealed tube, a Göbbel mirror and 0.5 mm pinhole collimator, and an Anton Paar TK1200 high temperature stage. The powder pattern was obtained from integration with a step size of 0.02° 2θ from 2D frames measured at 30 cm detector distance and a 10 min exposition time. The isolated single crystals were dried and ground using a mortar and pestle and placed on the heating stage prior to XRD analysis. Artificial aging under high relative humidity was conducted as described below.

Mössbauer Studies. ^{57}Fe Mössbauer spectra were recorded from powdered samples with a constant acceleration MS1200 Ranger Scientific, Inc. spectrometer and an ∼1.85 GBq ^{57}Co/Rh source. The iron density relating to the sample thickness was about 10 mg/cm^3 Fe. The line width of the α-Fe calibration spectrum at room temperature was 0.29 mm/s. Data were analyzed by a constrained least-squares fit to Lorentzian-shaped lines using the Recoil software.[36]

XPS Studies. XPS studies were conducted on a Kratos Axis 165 XPS spectrometer operating in hybrid mode using monochromatic Al Kα radiation at 280 W. Survey spectra and high-resolution spectra were collected with pass energies of 160 and 20 eV, respectively. Charge neutralization was required to minimize sample charging. Peak fitting was done after application of a Shirley background using 30% Lorentzian, 70% Gaussian product function.

DFT Calculations. All-electron density functional theory (DFT) calculations were performed on the $Fe(C_7O_5H_3)$ and $Fe(C_7O_5H_3)\cdot H_2O$ crystals using DMOL3 in the Accelrys Materials Studio (V.7) simulation package.[37,38] Electronic exchange and correlation effects were treated within the generalized gradient approximation in the Perdew−Burke−Ernzerhof (PBE) parametrization.[39] Double numerical plus polarization basis-set were used for the expansion of the electronic wave functions. A Monkhorst−Pack scheme with 3 × 3 × 2 k-points was used to sample the Brillouin zone and all calculations were done in a spin-polarized mode. Atomic positions were optimized with the unit cell parameters held to their experimental values; forces and total energy were converged to 0.002 Ha/Å and 10^{-5} Ha, respectively. All computations were conducted in the spin polarized mode.

Raman Studies. The 633 nm Raman data was collected using a Horiba Jobin Yvon LabRam Aramis confocal Raman spectrometer and 785 nm Raman data was collected using a Renishaw InVia Raman system outfitted with a Leica DM2500 microscope, CCD detector, and notch filters. The 633 nm spectra were calibrated to the 520.7 cm^{-1} line of Si. The data was collected with a 50× or 100× objective, a 600 l/mm grating and power at the sample of ∼0.09 mW. The 785 nm spectra were calibrated to the 520.5 cm^{-1} line of Si and collected at room temperature using a 1200 l/mm grating, and a 20×, 50×,

DOI: 10.1021/acs.analchem.6b00088
Anal. Chem. XXXX, XXX, XXX−XXX

or 100× objective. *In situ* Raman studies on historical documents were conducted with the same system with the aid of a proprietary macrosampling arm with a 20× objective that extended out over the object. Power at the samples was limited to 0.08−0.25 mW, depending on the objective; no change in the sample spectra from thermal damage was recorded in this range.

Artificial Aging. Select Fe(III) gallate crystals and IGI-ppt samples were artificially aged and studied by XRD and Raman spectroscopy. For artificial aging of the crystals under relatively high humidity, a heating stage was placed inside the sampling chamber of the XRD or Raman instrument. The stage was heated to 100 °C with a beaker of deionized water placed in the compartment for 1 h to create a humid environment. In the case of the Fe(III) gallate crystals, 633 nm Raman spectra were collected at selected heating intervals. For dry aging of the IGI-ppt, a small amount of sample was heated overnight at 150 °C in a conventional heating oven, followed by collection of the Raman spectra at room temperature.

RESULTS AND DISCUSSION

In this study, we employed a simplified system involving reactions between $FeSO_4{\cdot}7H_2O$ and gallic acid to study IGI chemistry without the complications of other historical ingredients, such as gum arabic. In a typical reaction for the preparation of the IGI-ppt, the reaction mixture quickly gives rise to a dark blue-black solution (eq 1). After a week of stirring in air, a very dark blue-black precipitate separates from solution with a 5−7% isolated yield. The supernatant remains blue-black in color. The pH of the solution drops from 2.8 to 1.8 during the course of the reaction, as measured by initial and final pH, indicating the gallic acid is deprotonated as it reacts with the iron ion. Elemental analyses (Galbraith Lab. Inc.) of washed IGI-ppt samples revealed an Fe to C ratio of 7:1; this ratio is independent of the initial molar ratio between the gallic acid and Fe(II) sulfate used to prepare the precipitate.

$$2Fe^{+2} + 2C_7O_5H_6 + 1/2O_2 \rightarrow 2Fe(C_7O_5H_3) + H_2O + 4H^+ \quad (1)$$

Preparations of IGI using a hydrothermal synthesis method result in the formation of black crystals in ∼10% yield. The pH of the supernatant drops from 4.50 to 3.50 after reaction. Similar reactions using buffers, different stoichiometries and concentrations routinely produce crystals that are mixed with varying amounts of amorphous IGI-ppt.

The insoluble black IGI-ppt is completely amorphous to X-rays but is composed almost exclusively of Fe(III) ions, intact gallate ligands, and water, as described below. Single crystal X-ray structures of crystals from different reaction batches show that they have the same trigonal $Fe(C_7O_5H_3){\cdot}xH_2O$ structure, space group $P3_121$, previously reported by Wunderlich[8−10] and Feller.[11] The structure is shown in Figure 1 and the crystal data are given in Table S1.

The disordered water content in the channels of the Fe(III) gallate framework structure varies from 1.5−3.2 (10−21% wt), but the structures are otherwise identical. Each gallate ligand is bound to three Fe atoms through the acid functional group and all three alcohol moieties (Figure 1a). The acid group and two of the three OH groups are deprotonated in the crystal lattice, giving the gallate ligand an overall −3 charge. Our single crystal structure is in agreement with the neutron structure of Feller, which shows that the para OH and one of the meta OH units

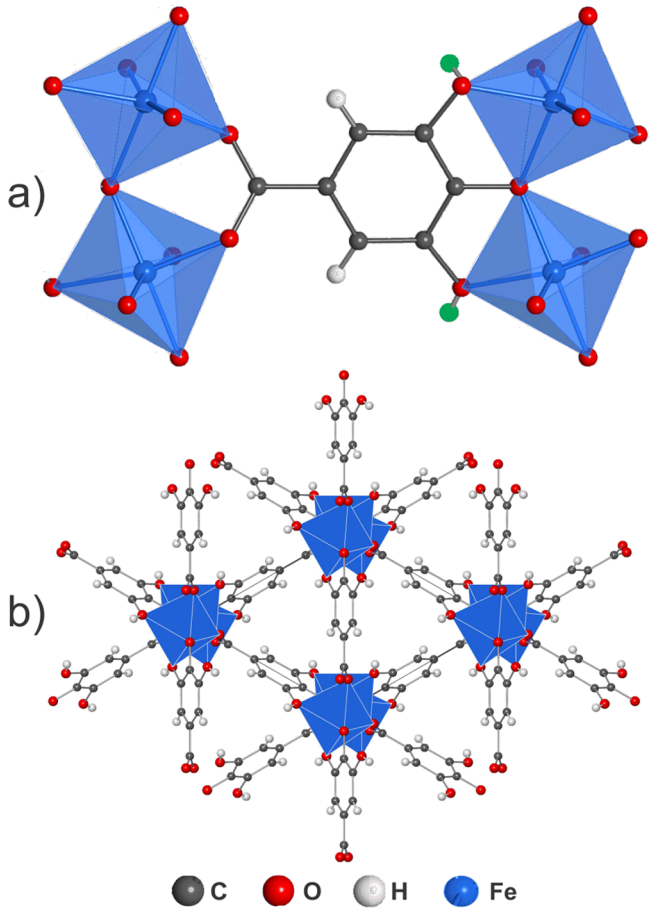

Figure 1. (a) Ball-and-stick rendering of $Fe(C_7O_5H_3) \cdot 3.22\ H_2O$ complex showing coordination of the gallate ligand. The meta-hydrogen atoms (green) are 50% occupied. (b) Framework structure viewed down the *c* axis. The water molecules in the channels have been omitted for clarity.

are deprotonated, whereas one meta OH remains protonated. This finding is in contrast to some earlier reports.[8−10,35,40] The meta OH proton is statistically disordered between the two meta OH sites in the lattice, which gives rise to a 50% H occupancy (green atoms, Figure 1a). The specific structural details have been described elsewhere[8−11] and will not be described further here. It is noteworthy that TGA (Figure S2) and FT-IR (Figure S3) of the IGI-ppt show that the water content is greater than in the Fe(III) gallate crystals.

The Fe(III) gallate crystals become amorphous in air or in water, typically over a 1 day to 2 week time frame. Loss of crystallinity can be accelerated by artificial aging of the samples above 100 °C and under high relative humidity. Powder XRD shows that as the Fe(III) crystals are artificially aged, they lose their crystallinity and eventually become completely amorphous (Figure S4). This is also exemplified by Raman spectroscopy, as discussed below.

Typical Mössbauer spectra of the Fe(III) gallate crystals and IGI-ppt collected at room temperature and liquid nitrogen temperature are shown in Figure 2. Mössbauer parameters are presented in Table S2. All the spectra are dominated by the Fe(III) high/spin paramagnetic doublet. In the case of the amorphous IGI-ppt samples (Figure 2a,b), the peaks are significantly broader, as expected for an amorphous material; spectra also show a small doublet characteristic of high/spin paramagnetic Fe(II) (4−8%). The relative area of this doublet

DOI: 10.1021/acs.analchem.6b00088
Anal. Chem. XXXX, XXX, XXX−XXX

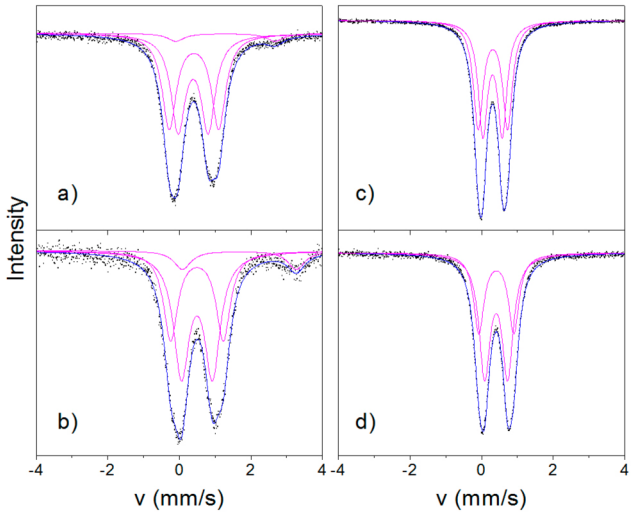

Figure 2. ^{57}Fe Mössbauer spectra for the freshly prepared the IGI-ppt collected at (a) room temperature and (b) LN_2 temperature and for Fe(III) gallate crystals collected at (c) room temperature and (d) LN_2 temperature.

is larger at liquid nitrogen temperature, as expected; this indicates a relative increase in the recoil free fraction for Fe(II) in a relatively soft organic matrix.[41] No sulfur was detected in these samples using XPS (Figure S5).

In contrast to the amorphous samples, Mössbauer spectra of the blue-black single crystals (Figure 2c,d) show they are composed entirely of Fe(III) ions with no detectable Fe(II) component. This finding indicates that the intense blue-black color of IGI initially originates from charge transfer bands and is not associated with intervalence charge transfer (i.e., Fe(II) ↔ Fe(III)), such as occurs in the well-known Prussian blue pigments ($Fe_4[Fe(CN)_6]_3{\cdot}xH_2O$ or $KFe[Fe(CN)_6]{\cdot}xH_2O$).[42,43]

The value of the Mössbauer parameters, as well as central shifts (CS) and quadrupole splitting (QS), indicate distorted octahedral coordination for Fe(II) in the IGI-ppt and distorted octahedral coordination for Fe(III) in both the crystalline and amorphous samples. Variation in the Mössbauer spectra with temperature is also characteristic of both cations, where CS is larger at liquid nitrogen temperature due to the second order Doppler shift, and QS is larger at low temperature. Although the latter phenomenon is less characteristic for Fe(III), it can indicate an increase in the degree of distortion. The Fe(III) doublet appears slightly asymmetric, even for the crystalline samples, and is thus fit with two doublets having different QS but similar CS, although the crystal structure indicates just one type of Fe(III) exists.

XPS data collected from the IGI-ppt and the $Fe(C_7O_5H_3){\cdot}xH_2O$ single crystals are essentially identical, which suggests that the composition and coordination environments of the crystalline and amorphous samples are equivalent. Figure 3 shows high-resolution XPS C 1s and O 1s data for samples of pure gallic acid, crystalline $Fe(C_7O_5H_3){\cdot}xH_2O$ and IGI-ppt. The C 1s spectrum of pure gallic acid (Figure 3a) is fit with peaks that have constrained areas based on the known 3:3:1 ratios of C−C (1), C−O (2), and O═C−O−H (3). The O 1s spectrum of gallic acid (Figure 3b) is fit using the same rationale (red numbers), showing the 4:1 ratio of sp^3 O (1) to sp^2 O (2), which is in excellent agreement with theoretical amounts of the different chemical environments in gallic acid.

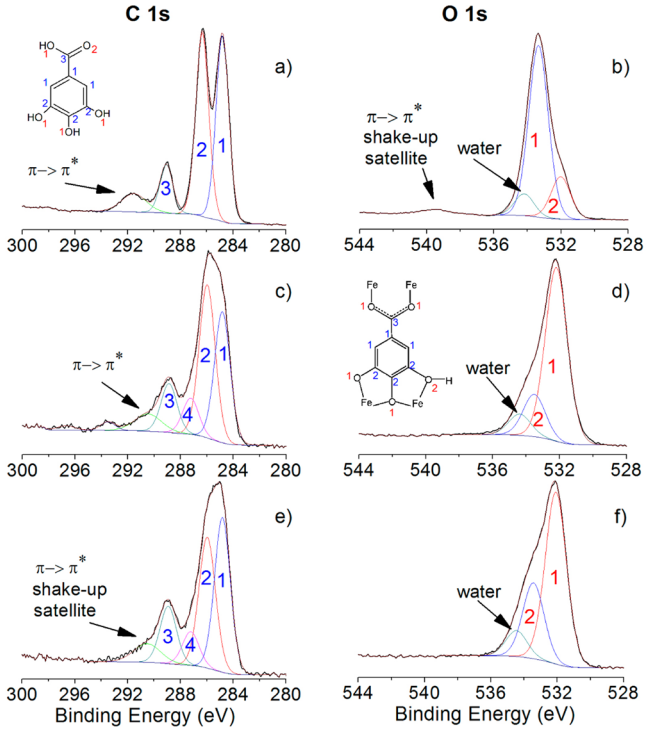

Figure 3. Carbon 1s (left) and oxygen 1s (right) XPS spectra for (a,b) gallic acid, (c,d) crystalline $Fe(C_7O_5H_3){\cdot}xH_2O$, and (e,f) amorphous IGI precipitate. Peak assignments for carbon (blue) and oxygen (red) bonds are shown in the insets corresponding to either gallic acid (top left) or Fe(III) gallate (middle right). Peak no. 4 in the carbon 1s spectra is associated with uncomplexed surface C−O species.

The C 1s and O 1s peaks additionally show the expected $\pi \rightarrow \pi^*$ shakeup satellites due to the aromatic ring and carbonyl oxygen in gallic acid, respectively. For reference purposes, Figure S6 shows the Fe 2p spectra the crystalline $Fe(C_7O_5H_3){\cdot}xH_2O$ and IGI-ppt.

The corresponding C 1s and O 1s XPS spectra for the $Fe(C_7O_5H_3){\cdot}xH_2O$ crystalline sample are shown in Figure 3c,d, respectively. The peak assignments are made with the aid of all-electron density functional theory (DFT) calculations on the $Fe(C_7O_5H_3)$ and $Fe(C_7O_5H_3){\cdot}H_2O$ complexes. Figure 4 shows

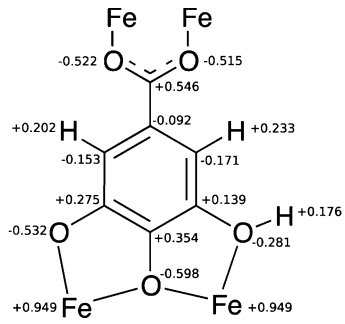

Figure 4. Calculated partial charges of the Fe(III) gallate crystal.

the calculated Mulliken partial charges[44] on the gallate ligand in the unhydrated $Fe(C_7O_5H_3)$ cell. Half of the meta hydrogens were given full occupation and all calculations were performed on the conventional cell containing three Fe-gallate ligand units. Additional calculations with a single H_2O in the unit cell channel show essentially no changes in the partial charges of

DOI: 10.1021/acs.analchem.6b00088
Anal. Chem. XXXX, XXX, XXX−XXX

the metal center or the gallate ligand. The 3:3:1 concentrations of C−C (1), C−O (2), and Fe(COO) (3) functional groups and the $\pi \rightarrow \pi^*$ shakeup peak are retained in the C 1s spectrum of the complex. An additional shoulder at 287.5 eV (peak no. 4) is associated with an uncomplexed surface C−O species. This feature likely arises from surface oxidation of samples. The 4:1 ratio of O 1s peaks in the gallic acid ligand is also retained in the $Fe(C_7O_5H_3)\cdot xH_2O$ complex; however, the relative binding energies of the peaks are reversed, so that the intensity of peak no. 4 is lower binding energy relative to the intensity of peak no. 1. The DFT calculated relative charge distributions show that four of the five oxygen atoms bear an ∼−0.55 charge, whereas the protonated phenoxide oxygen is significantly more positive at −0.28 (Figure 4). The high negative charges give rise to peaks of lower O 1s binding energies, which is in excellent agreement with the observed 4:1 peak ratio and energy ordering in O 1s spectra. The increased O 1s intensity at ∼533 eV and the increase in ratio of peak 4:2 in the C 1s XPS spectra of the IGI-ppt (Figure 3e,f) indicate a larger proportion of uncomplexed surface C−O species compared to the crystals.

The 633 and 785 nm Raman spectra of the iron-gallate samples (Figure 5, Figure 6, and Table S3) provide further

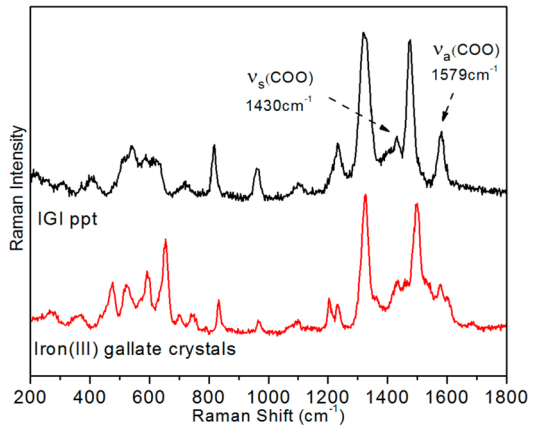

Figure 5. Raman spectra of (top) IGI-ppt and (bottom) Fe(III) gallate crystals, acquired with a 633 nm excitation source.

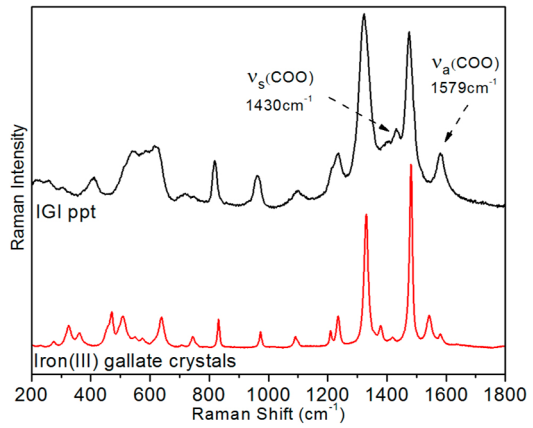

Figure 6. Raman spectra of (top) IGI-ppt and (bottom) Fe(III) gallate crystals, acquired with a 785 nm excitation source.

support for the Fe(III) iron gallate structure in terms of both the functionality and sample crystallinity.[45−47] For example, 785 nm Raman spectra of the $Fe(C_7O_5H_3)\cdot xH_2O$ crystalline samples contain sharp and well-defined peaks, consistent with the high degree of crystallinity and the distinct chemical environments of the functional units (Figure 6, bottom). In contrast, the IGI-ppt (Figure 5 and Figure 6, top) shows broader peaks with some slight shifting, but the primary features remain intact. In all cases, spectra of IGI-ppt samples show they contain all of the functional groups of the parent, crystalline structure, which is dominated by the C−C and C−O vibrational modes of the phenolic rings. Specifically, the stretching modes of the coordinated COO near 1579 cm^{-1} (asymmetric) and 1430 cm^{-1} (symmetric) are observed in the Raman and FT-IR spectra (Figure S3) of the crystalline samples and the amorphous IGI materials. The peak positions and separations (∼149 cm^{-1}) are also consistent with the bridging carboxylate functionality observed in the crystal structure.[48]

The crystalline to amorphous transition is clearly delineated through Raman spectra taken from progressively aged crystals (100 °C, humid conditions), as shown in Figure 7a−c. Furthermore, spectra of the artificially aged crystals appear indistinguishable from those of the amorphous IGI-ppt after dry aging overnight at 150 °C (Figure 7d).

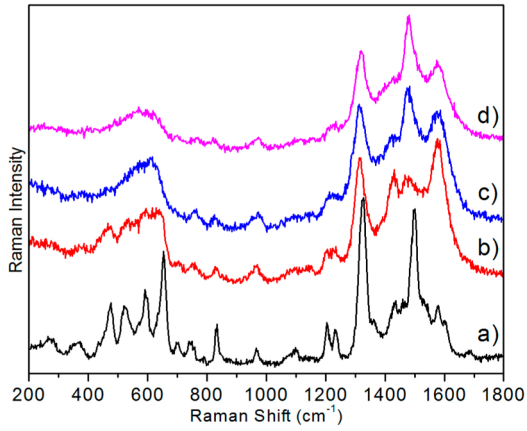

Figure 7. Raman spectra of the IGI ppt and of the IGI crystals with artificial aging, acquired with a 633 nm excitation source: (a) IGI crystals at room tempearture; (b) IGI crystals heated at 100 °C for 15 min; (c) IGI crystals heated at 100 °C for 38 min; and (d) IGI ppt heated at 150 °C overnight.

Characteristic 785 nm Raman spectra from the model samples (Figure 8a,b) have been compared to spectra collected from the ink and paper of a large number of historical IGI-containing documents from the 17th−19th centuries. In Figure 8, we show typical 785 nm Raman spectra recorded from a random, hand-written manuscript from 1842 (Figure 8c), and George Washington's hand-written "Extracts and Notes on Agriculture" (1760−1799) in the collection of the Library of Congress (Figure 8d and Figure 9). In both cases, the documents have not been treated or chemically altered as far as we know. Qualitative XRF analysis of the historical materials examined here show that Fe, K, and S are the dominant heavy elements in these inks. While trace Zn or Ca contaminants are also possible (Table S4), they were not detected in our experiments. The presence of K and S in both cases is consistent with lack of aqueous treatment. The dominant features of historical IGI spectra can be ascribed to the $Fe(C_7O_5H_3)$ functional unit and are virtually identical to the spectra of the artificially aged model IGI compounds. In particular, the 1430 and 1579 cm^{-1} symmetric and asymmetric

DOI: 10.1021/acs.analchem.6b00088
Anal. Chem. XXXX, XXX, XXX−XXX

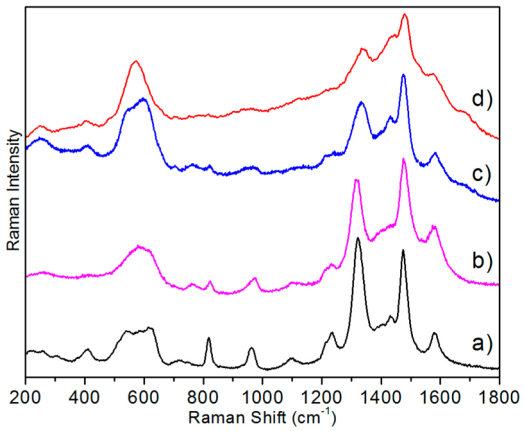

Figure 8. Raman spectra of the IGI-ppt before and after artificial aging compared with historical documents, acquired with a 785 nm excitation source: (a) IGI-ppt, (b) IGI-ppt dry aged overnight at 150 °C, (c) ink on a random manuscript dated 1842, and (d) ink on George Washington's *Extracts and Notes on Agriculture* (1760−1799, George Washington Papers, Manuscript Division, Library of Congress, Washington, DC).

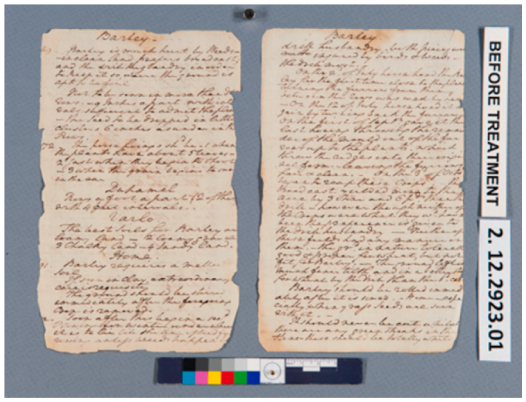

Figure 9. Image of two leaves from President George Washington's "Barley Notes" (George Washington, 1760−1799, *Extracts and Notes on Agriculture*, George Washington Papers, Manuscript Division, Library of Congress, Washington, DC). Photo Credit Julie Biggs.

Fe(COO)Fe binding mode vibrations are clearly present in all samples, indicating that the carboxylate groups remain intact in the ink structures. These results are in excellent agreement with the spectroscopic studies described above and show that the artificially aged amorphous product of the crystalline sample is virtually identical to the artificially aged amorphous IGI-ppt samples prepared under ambient conditions and the ink present in historical documents. While Raman spectra of historical IGI have been reported, these results show for the first time that the spectral characteristics of typical historical IGIs correspond to pure, synthetic IGI-ppts and crystals.

CONCLUSIONS

We show here that the $Fe(C_7O_5H_3)\cdot xH_2O$ IGI colorant can be prepared from the authentic $FeSO_4$ and gallic acid precursors in both crystalline and amorphous forms and that these products are spectroscopically very similar. Collectively, these data show that the IGI-ppt, crystalline $Fe(C_7O_5H_3)\cdot xH_2O$, and historical examples of IGI have the same basic colorant in terms of composition, functional groups, and initial iron oxidation state. Specifically, the carboxylate group of the gallic acid is clearly present in the crystalline and amorphous iron gallate complex (XPS, Raman, elemental analysis) and the iron is initially in the +3 oxidation state (Mössbauer, XPS). The artificially aged, analytically pure samples contain both Fe(II) and Fe(III), indicating that redox occurs over time, which can easily be accommodated in the $M(gallate)\cdot xH_2O$ structure type. Feller and Cheetham have shown that divalent metal ions, such as Mn(II), Co(II), and Ni(II), all form metal gallates that are isomorphic to the $Fe(C_7O_5H_3)\cdot xH_2O$ structure and differ only in the degree of protonation of the gallic acid ligand.[11] Both the pure Fe(III) gallate crystal and the IGI ppt made from historically relevant ingredients, i.e., iron sulfate and gallic acid, have the same initial blue-black color to the naked eye. However, a mixed-valent Fe(II)−Fe(III) complex in the aged samples could have additional intervalence charge transfer, augmenting the color of the ink, similar to Prussian blue pigments.[42,43]

The strong similarities in the XPS and Raman spectra of model samples and historical inks also indicate that the coordination modes of the gallate ions in all cases are the same, i.e., the structural units in the $Fe(C_7O_5H_3)\cdot xH_2O$ remain intact. It is unclear at present what causes the meta-stability of the crystal lattice that results in the amorphous structure. It appears that the degree of hydration and the ordering of water and gallate can vary in these structures.[11] The loss of water or the onset of reduction [Fe(III) → Fe(II)] could drive the instability. Further studies are in progress.

ASSOCIATED CONTENT

Supporting Information

The Supporting Information is available free of charge on the ACS Publications website at DOI: 10.1021/acs.analchem.6b00088.

Additional spectroscopic spectra and Mössbauer data (PDF)

Crystallographic (CCDC 1407610) data; full crystallographic data can be found in CCDC, file number 1407610 (CIF)

AUTHOR INFORMATION

Corresponding Authors

*E-mail: lbrostoff@loc.gov.

*E-mail: kgaskell@umd.edu.

*E-mail: eichhorn@umd.edu.

Notes

The authors declare no competing financial interest.

ACKNOWLEDGMENTS

We thank the Library of Congress, Howard Hughes Medical Institute for an HHMI Fellowship (S.K.G.), and the University of Maryland for financial support.

REFERENCES

(1) Shahani, C. J.; Hengemihle, F. H. In *Historic Textile and Paper Materials: Conservation, Degradation, and Characterization of Paper*; Needles, H. L., Zeronian, H. L., Eds.; Advances in Chemistry Series, Vol. *212*, American Chemical Society: Washington, DC, 1986; pp 387−410.

(2) Neevel, J. G. *Restaurator* **1995**, *16* (3), 143.

(3) Strlic, M.; Selih, V. S.; Kolar, J. In *Iron Gall Inks: On Manufacture Characterization Degradation and Stabilisation*; Kolar, J., Strlic, M., Eds.; National and University Library: Ljubljana, Slovenia, 2006; pp 173−180.

DOI: 10.1021/acs.analchem.6b00088
Anal. Chem. XXXX, XXX, XXX−XXX

(4) Kolar, J.; Strlic, M. In *Iron Gall Inks: On Manufacture Characterization Degradation and Stabilisation*; Kolar, J.; Strlic, M., Ed.; National and University Library: Ljubljana, Slovenia, 2006; pp 181−194.
(5) Steemers, T. In *Iron Gall Inks: On Manufacture Characterization Degradation and Stabilisation*; Kolar, J.; Strlic, M., Ed.; National and University Library: Ljubljana, 2006; pp 20−24.
(6) Potthast, A.; Henniges, U.; Banik, G. *Cellulose* **2008**, *15* (6), 849.
(7) Henniges, U.; Banik, G.; Reibke, R.; Potthast, A. *Macromol. Symp.* **2008**, *262*, 150.
(8) Wunderlich, C. H. *Geschichte und Chemie der Eisengallustinte und Struktur des Eisen(III)-Gallussäure-Komplexes*. Ph.D. Dissertation, Rheinischen Friedrich-Wilhelms-Universität Bonn, Bonn, Germany, 1990.
(9) Wunderlich, C.-H.; Weber, R.; Bergerhoff, G. *Z. Anorg. Allg. Chem.* **1991**, *598*, 371.
(10) Wunderlich, C.-H. *Restauro* **1994**, 414−421.
(11) Feller, R. K.; Cheetham, A. K. *Solid State Sci.* **2006**, *8*, 1121.
(12) Thompson, D. V. *The Materials and Techniques of Medieval Painting*; Dover: New York, 1956.
(13) Sistach, M. C.; Gibert, J. M.; Areal, R. *Restaurator* **1999**, *20*, 151.
(14) James, C. In *The Postprints of the Iron Gall Ink Meeting*; Brown, A. J. E., Ed.; The University of Northumbria: Newcastle, U.K., 2001; pp 13−22.
(15) Stijnman, A. In *Iron Gall Inks: On Manufacture Characterization Degradation and Stabilisation*; Kolar, J., Strlic, M., Eds.; National and University Library: Ljubljana, Slovenia, 2006; pp 25−67.
(16) Zetzsche, F.; Vieli, G.; Lilljequist, G.; Loosli, A. *Ann. Chem.* **1924**, *435*, 233−264.
(17) Darbour, M.; Bonassies, S.; Flieder, F. In *Preprints of the ICOM-CC 6th Triennial Meeting*, Ottawa, Canada; van Asperen de Boer, J. R. J., Ed.; ICOM: Paris, France, 1981; Vol. 3, 3, pp 1−14.
(18) Sistach, M. C. In *Preprints of the ICOM-CC 9th Triennial Meeting*, Dresden, Germany; Grimstad, K., Ed.; ICOM: Los Angeles, CA, 1990; Vol. 2, pp 489−494.
(19) Daniels, V. In *The Postprints of the Iron Gall Ink Meeting*; Brown, A. J. E., Ed.; The University of Northumbria: Newcastle, U.K., 2001; pp 31−36.
(20) Arpino, P.; Moreau, J. P.; Oruezabal, C.; Flieder, F. *J. Chromatogr.* **1977**, *134*, 433.
(21) Flieder, F. *Restaurator* **1981**, *5*, 57.
(22) Powell, H. K. J.; Taylor, M. C. *Aust. J. Chem.* **1982**, *35* (4), 739.
(23) Krekel, C. *International Journal of Forensic Document Examiners* **1999**, *5*, 54.
(24) Krekel, C. In *Tintenfraßschäden und ihre Behandlung*; Banik, G., Weber, H., Eds.; W. Kohlhammer: Stuttgart, Germany, 1999; pp 25−36.
(25) Yamahara, R.; Ogo, S.; Masuda, H.; Watanabe, Y. *J. Inorg. Biochem.* **2002**, *88*, 284.
(26) Perron, N. R.; Brumaghim, J. L. *Cell Biochem. Biophys.* **2009**, *53*, 75.
(27) Neevel, J. G. In *The Postprints of the Iron Gall Ink Meeting*; Brown, A. J. E., Ed.; The University of Northumbria: Newcastle, U.K., 2001; pp 125−131.
(28) Neevel, H. In *Iron Gall Inks: On Manufacture Characterization Degradation and Stabilisation*; Kolar, J., Strlic, M., Eds.; National and University Library: Ljubljana, Slovenia, 2006; pp 147−172.
(29) Rouchon, V.; Duranton, M.; Burgaud, C.; Pellizzi, E.; Lavedrine, B.; Janssens, K.; de Nolf, W.; Nuyts, G.; Vanmeert, F.; Hellemans, K. *Anal. Chem.* **2011**, *83*, 2589.
(30) Reißland, B. *Restaurator* **1999**, *20*, 167.
(31) Rouchon-Quillet, V.; Remazeilles, C.; Bernard, J.; Wattiaux, A.; Fournes, L. *Appl. Phys. A: Mater. Sci. Process.* **2004**, *79*, 389.
(32) La Camera, D. *J. Am. Inst. Conserv.* **2007**, *46*, 153.
(33) Maitland, C. L. *Book and Paper Group Annual* **2009**, *28*, 37.
(34) Tse, S.; Guild, S.; Gould, A. *Journal of the Canadian Association for Conservation* **2012**, *37*, 3.
(35) Zaccaron, S.; Ganzerla, R.; Bortoluzzi, M. *J. Coord. Chem.* **2013**, *66* (10), 1709.
(36) Lagarec, K.; Rancourt, D. G. *Recoil-Mössbauer Spectral Analysis Software for Windows*, version 1.0; University of Ottawa: Ottawa, Canada, 1998.
(37) Delley, B. *J. Chem. Phys.* **1990**, *92*, 508.
(38) Delley, B. *J. Chem. Phys.* **2000**, *113*, 7756.
(39) Perdew, J. P.; Burke, K.; Ernzerhof, M. *Phys. Rev. Lett.* **1996**, *77*, 3865.
(40) Zaccaron, S.; Bortoluzzi, M.; Ganzerla, R. *Sciences at Ca' Foscari* **2013**, *2* (1), 58.
(41) Dickson, D. P.; Berry, F. J. In *Mössbauer Spectroscopy*, 1st ed.; Cambridge University Press: Cambridge, U.K., 1986.
(42) Dunbar, K. R.; Heintz, R. A. *Prog. Inorg. Chem.* **1997**, *45*, 283.
(43) Berrie, B. H. In *Artists' Pigments: A Handbook of Their History and Characteristics*, Vol. 3; FitzHugh, E. W., Ed.;Oxford University Press: New York, 1977; pp 191−218.
(44) Segall, M. D.; Pickard, C. J.; Shah, R.; Payne, M. C. *Mol. Phys.* **1996**, *89*, 571.
(45) Hartl, F.; Vlcek, A., Jr. *Inorg. Chem.* **1996**, *35*, 1257.
(46) Billes, F.; Mohammed-Ziegler, I.; Bombicz, P. *Vib. Spectrosc.* **2007**, *43*, 193.
(47) Lee, S.; Mahon, P. J.; Creagh, D. C. *Vib. Spectrosc.* **2006**, *41*, 170.
(48) Deacon, G. B.; Phillips, R. J. *Coord. Chem. Rev.* **1980**, *33*, 227.

DOI: 10.1021/acs.analchem.6b00088
Anal. Chem. XXXX, XXX, XXX−XXX